IEEE Access
Multidisciplinary | Rapid Review | Open Access Journal

Received November 17, 2021, accepted November 30, 2021, date of publication December 3, 2021,
date of current version December 15, 2021.

Digital Object Identifier 10.1109/ACCESS.2021.3132383

Allied Power Constraint Optimization and Optimal Beam Tracking Schemes for Mobile mmWave Massive MIMO Communications

JOYDEV GHOSH[1], (Member, IEEE), IN-HO RA[2], (Member, IEEE), SAURABH SINGH[3], HÜSEYIN HACI[4], KHALED A. AL-UTAIBI[5], (Member, IEEE), AND SADIQ M. SAIT[6], (Senior Member, IEEE)

[1]School of Computer Science and Robotics, Tomsk Polytechnic University, 634050 Tomsk, Russia
[2]School of Computer, Information and Communication Engineering, Kunsan National University, Gunsan 54150, South Korea
[3]Department of Industrial and Systems Engineering, Dongguk University, Seoul 04620, South Korea
[4]Department of Electrical and Electronics Engineering, Near East University, 99138 Mersin, Turkey
[5]Computer Science and Software Engineering Department, University of Hail, Hail 53962, Saudi Arabia
[6]Department of Computer Engineering, King Fahd University of Petroleum and Minerals, Dhahran 31261, Saudi Arabia

Corresponding author: In-Ho Ra (ihra@kunsan.ac.kr)

This work was supported in part by the Korean Institute of Energy Technology Evaluation and Planning (KETEP) by the Korean Government through the Ministry of Trade, Industry, and Energy (MOTIE) under Grant 20194010201800, and in part by the National Research Foundation of Korea (NRF) Grant by the Korean Government through the Ministry of Science and ICT (MSIT) under Grant 2021R1A2C2014333.

ABSTRACT The fifth generation (5G) networks and internet of things (IoT) promise to transform our lives by enabling various new applications from driver-less cars to smart cities. These applications will introduce enormous amount of data traffic and number of connected devices in addition to the current wireless networks. Thus 5G networks require many researches to develop novel telecommunication technologies to accommodate these increase in data traffic and connected devices. In this paper, novel power constraint optimization and optimal beam tracking schemes are proposed for mobile mmWave massive MIMO communications. A recently published novel channel model that is different from other widely used ones is considered. The channel model considers the number of clusters and number of rays within each cluster as varying due to user mobility. The proposed power constraint optimization scheme harmonizes conventional total power constraint (TPC) and uniform power constraint (UPC) schemes into a new one called allied power constraint (APC) that can significantly improve the system performance in 5G networks while achieving fairness among users. TPC and UPC have major drawbacks with respect to fairness and achieving quality-of-service (QoS) for users in dense networks. Thus APC aims to harmonize TPC and UPC by adjusting each antenna element's constraint to adapt for some power resilience to a specific antenna element, hence proposing an intermediate solution between the two extreme case power constraint optimization schemes. Three optimal beam tracking schemes: (i) conventional exhaustive search (CES), (ii) multiobjective joint optimization codebook (MJOC), and (iii) linear hybrid combiner (LHS) scheme, have been provided for the mobile mmWave massive MIMO system with the proposed APC scheme. For the proposed APC scheme a comprehensive performance analysis is provided and compared with TPC and UPC. Spectral efficiency (SE), bit-error-rate (BER), Jain's fairness index, channel occupancy ratio (COR) and instantaneous interfering power metrics are investigated. It has been shown that the proposed scheme can significantly outperform conventional schemes.

INDEX TERMS Power constraint schemes, beam tracking schemes, signal to interference plus noise ratio (SINR), channel occupancy ratio (COR), bit error rate (BER), channel state information (CSI), multiple-input-multiple-output (MIMO), 5G.

The associate editor coordinating the review of this manuscript and approving it for publication was Wenjie Feng.

I. INTRODUCTION

Internet of Things (IoT) and Cloud-based services have lead to a tremendous increase in wireless data traffic and it is

expected that the total number of mobile subscribers will reach 5.7 billion by 2023 (which is 71 percent of current global population) [1], [2]. In order to handle this increase in traffic, novel communication technologies that can work in harmony and significantly improve system capacity are needed at every protocol layer of communication systems. The fifth generation (5G) networks promise to provide these novel technologies. 5G technology is driven by eight specification requirements, which are up to 100× data rate improvement, 1000× bandwidth increase per unit area, 100× number of connected devices per unit area and 90% reduction in network energy usage compared to the fourth generation (4G) networks, 1 millisecond latency, up to 10 year battery life for low power IoT device, 100% coverage and 99.999% availability. With the aim to achieve these requirements and as a fundamental and enabling layer to all the higher layers, researches at physical layer technologies for next generation of communications gain a big trajectory. Millimeter wave (mmWave) technology is both a major research area and an enabling technology for the physical layer of future telecommunication systems. This is because, by significantly decreasing the wavelength of transmitted signals, mmWave technology enables the realization of massive MIMO communications. Beamforming in MIMO systems is a technique that is employed to focus a wireless signal towards a specific receiving device. This can increase overall system's energy efficiency and reduce cost due to lower power consumption and amplifier costs of massive MIMO systems [3]. Multi-beamforming techniques are popular research topics that many researches study to enhance the performance gain by single-beamforming technology [4]. Since today's end users are highly mobile, beams that are formed needs to be able to track mobile users so that wireless signals can be focused onto the users' latest position accurately. In [5], it has been shown that when the beam handoff due to users' mobility is not appropriately handled there is significant degradation in the quality of service (QoS) users' perceive. Accordingly a beam tracking technique with link robustness was introduced in this paper to deal with the issue of beam handoff in mmWave communications in order to provide optimal beam coverage for mobile users. Further, with the user mobility the mmWave channel undergoes Doppler frequency shift and the number of clusters and number of rays generated from each cluster varies. This mmWave channel model has only been considered recently by [6] that is novel and different from other widely used models. In this paper we studied and proposed schemes for this novel channel model.

Another crucial aspect in multi-user beamforming communications is the transmission power management to achieve reliable and ultra-high speed communications [7]. Conventional power constraint based optimization, total power constraint (TPC) and uniform power constraint (UPC) schemes, have major drawbacks such as UPC not being able to satisfy users' QoS when the network become densely populated and TPC not being able to achieve fairness among users while maximizing the system throughput [8], [9]. Therefore to address these open challenges this paper proposes a novel power constraint optimization and optimal beam tracking schemes for mobile mmWave massive MIMO communications with a recently proposed channel model.

A. RELATED WORK

To overcome the limitation of narrowband systems design with hybrid precoding, authors in [10] proposed a novel beam tracking scheme suitable for wideband systems by incorporating delay-phase precoding and applying the beam zooming concept. This scheme not only decreases beam training overhead, but also offers multiple user tracking rather than tracking only one user in a time slot. Researchers in [11] and [12] showed work on extended Kalman filter (EKF) to track channel state based on the linearization mechanism subject to the channel state estimation and the covariance magnitude. But as it is well known that in most of the cases the channel models are nonlinear to match with practical scenarios and the Jacobian matrices correspond to directional sounding beam, hence minimum deviation from main design limitations in the EKF operation may cause unstable performance with large computational overhead. For this reason, [13] proposed unscented Kalman filter (UKF) with the intractability of recursive Bayesian estimation that does not depend on a Jacobian matrix and presented that the UKF is a better tracking scheme compared to that of the EKF. According to [14], based on extended Kalman filter (EKF) incorporating a monopulse signal is an effective beam tracking scheme for the moving object in the unmanned aerial vehicles (UAVs) to manage the challenges of mobility and frequent channel disconnection and also shown that it is even better compared to other conventional schemes [11], [15], [16]. By considering UAV position and attitude estimation with machine learning (ML), an efficient beamwidth control based beam tracking approach was proposed in [17], [18] for optimal beam pair selection. Besides this, [19] presented a beam tracking scheme based on KF with the use of monopulse signal, rather than a beam-formed signal, that can compute accurate angular estimation to deal with the issue of vehicle perturbations in UAV communication. There are two algorithms that can be seen in the literature based on imperfect angle-of-arrival (AoA) and angle-of-departure (AoD) such as least mean squares (LMS) and bidirectional LMS (BiLMS) algorithms, and LMS is shown to be the better choice compared to the comprehensively used EKF algorithm. Thereafter, by following the results demonstration BiLMS proved to be the best compared to both LMS and EKF according to [20]. As shown in [21], a useful blind beam tracking approach with particle filter can be an effective scheme to address the challenges of excessive overhead due to consideration of more training sequences according to IEEE 802.11 ad and beam misalignment, respectively. Authors in [22] proposed an advanced beam tracking algorithm which does not require spatial scanning at the time of data transmission.

According to [23], the spectral occupancy measurement can be done by assuming channel based occupancy and frequency based occupancy. Authors in [24] showed that frequency based occupancy estimation has higher value compared to channel based occupancy estimation. Although, frequency based occupancy technique is recommended only for estimating in the field of sensing, but needs to be improved with the help of multiple tools to achieve higher values. So far occupancy was generally measured by assuming the received signal strength (RSS) at the time of observation whether to go higher or lower than the threshold and it can be expressed as a percentage [25]. These days spectrum utilization is generally done with the consideration of duty cycle (DC) and channel occupancy ratio (COR) metrics. The COR signifies that a channel is considered to be occupied if the energy measured by energy detector is higher than the threshold and it also provides an indication that a channel is occupied if small portion of the channel is already shared with other users. Even though the property of the COR has a great potential in reducing interference and help protect existing users, as of today most of the work done on spectrum utilization is based on considering the metric DC. The modern days traffic can be handled by considering wireless local area network (WLAN) COR estimation scheme which signifies the channel occupancy with sweep time in time domain [26]. However, [27] proposed that spectral sweeping energy detection (ED) scheme based on fast fourier transform (FFT) for the low RSS is better in terms of accuracy compared to WLAN COR estimation.

The sparse vector coding (SVC) is recently considered as one of the strong candidates for improving ultra-reliable low-latency (URLL) communication. Nowadays SVC utilizes index modulation (IM) that helps to pass on extra information bits, whereas earlier SVC was used with the utilization of virtual digital domain (VDD) and compressed sensing (CS) algorithms. Authors in [28] with the help of simulation results showed that IM-SVC can provide much better BER performance compared to the algorithm based SVC. The BER upper bound is derived analytically for orthogonal frequency division multiplexing (OFDM) with index modulation (OFDM-IM) in [29] and maximum likelihood (ML) detection OFDM-IM in [30], respectively. Although non-iterative neural network decoder (NND) is also very popular in URLL networks, it has an unsatisfactory BER performance. Therefore, [31] proposed a residual learning denoiser (RLD) in order to have better signal-to-interference plus-noise ratio (SINR) and symbol-error-rate (SER). In [32]–[34], comparative studies on BER metric for the different spatial modulation (SM) based schemes have been introduced. The successive user detection (SUD)-SM is reasonably good with low decoding complexity at the cost of BER, whereas another modified version SUD with a little higher complexity can provide improved BER and SM-sparse code multiple access (SCMA) with low complexity is shown to have a near-optimum BER. The block diagonalization multi-user SM (BD-MU-SM) shown to be the best in achieving a balanced data-rate and BER performance. Considering the challenges of the non-linear distortions with the use of high power amplifier (HPA), the BER in NOMA-OFDM networks is evaluated by theoretical analysis along with Monte Carlo simulation [35]. The role of deep neural networks as a machine learning approach in the learn iterative search algorithm (LISA) in [36] for the purpose of MIMO system is shown to be very effective and efficient for BER performance. In [37], the precoded OFDM (P-OFDM) technique that takes into account carrier frequency offset (CFO) is shown to provide better BER than conventional OFDM. The authors in [38] worked on independent component analysis (ICA) scheme based on maximum likelihood (ML) principle rather than just conventional ICA scheme to minimize BER. In the multiple antenna ambient backscatter scenarios, the characterization of BER was established in [39] and [40] by the energy detector and the maximum-eigenvalue detector. Employing likelihood ratio test maximum-eigenvalue detector is shown to outperform other energy detectors. To overcome the issue of time asynchronization due to high-mobility, the effectiveness of the linear programming (LP) decoder with the ML application property is shown to be a very good choice to achieve close-to-optimal BER [41]. Sparse code spreading-aided multi-carrier differential chaos shift keying (SCS-MC-DCSK) transceiver is proposed by [42] and shown to provide reliable communications under different channel conditions. Reference [43] compared the performance of filter shape index modulation (FSIM) with quadrature amplitude modulation (QAM) and quadrature phase shift keying (QPSK) in terms of filter index error and BER lower bound. It is shown that FSIM can provide better performance than QAM and QPSK. To mitigate error propagation, the application of the soft BER stopping rule is employed in the braided convolutional codes (BCCs) in [44] rather than obsolete BCCs with iterative decoding thresholds, minimum distance characteristics and their BER. The use of the soft BER stopping rule is shown to be helpful to decrease the computational complexity with similar BER performance. In [45] the asymptotic BER performance of reconfigurable intelligent surfaces (RIS) model is mathematically derived and confirmed via Monte Carlo simulation. For the purpose of channel impairments, the proposed design in [46] for vehicle to everything (V2X) communication had become very effective for higher-order modulation with more than 85% improved BER and accuracy of mean-squared error (MSE) lesser than 10^{-4}. A new BER expression for smart utility networks (SUN) with WLAN interferers is developed in [47] and shown to be time dependent. The data-aided joint superimposed pilot (J-SIP) scheme for mmWave MIMO-OFDM channel model had been investigated in [48] for beam tracking and channel state information (CSI) acquisition through the multiple measurement vector (MMV) sparse Kalman filtering and the joint Kalman filtering respectively, which turned out to provide better MSE of the channel estimation and BER.

Furthermore, since the impact of multipath-fading creates difficulty in producing low-latency links, MIMO can offer low-latency links by reducing fading effects in the air interface. However, large antenna arrays used in massive MIMO makes its implementation computationally expensive with high energy consumption due to requirement of large RF chains. Although, beamforming technology at massive MIMO can improve the spectral efficiency even more through optimizing training sequences to maximize the carrier-to-interference power ratio. The use of analog/digital beamformers that reduces the size of up/down conversion chains are emerging as a promising solution to such challenges. For digital architecture, beamforming can be achieved with beam training. Exhaustive search algorithm (ESA) [49] searches all the possible beam combinations to identify the optimum beam pair. As the codebook size increases, the complexity of ESA increases exponentially and the computational complexity becomes prohibitive. Thus, ESA can only be used for small codebooks. Reference [50] proposed a low complexity beam tracking method for mobile mmWave communications that requires to train only one beam pair to track a propagation path. In fast changing environments [50] achieved better performance than full scan beam tracking systems. Reference [49] proposed a beam training technique that uses a simplex-based global direct search optimization method to track strong beam stream for mmWave communications. The performance has been shown to be near-optimal with lower search complexity compared to ESA. Reference [51] proposed a Kronecker-separable extension to the linearly constrained minimum variance (LCMV) filter beamformers to significantly improve the computational efficiency. It has been shown that the proposed scheme outperforms classical LCMV beamformers especially in the low signal to noise ratio (SNR) regime. Reference [52] proposed a near-optimal codebook-based beam training technique for mmWave communication systems that uses a variant of global direct search algorithm where the searching algorithm tracks the strong beam by using expansive, rotational, or shrinkage translation of the solution simplex. It has been shown that in multipath channels there are multiple local optima and this scheme may converge to a local optima. This problem was addressed by [16] through iterating their algorithm multiple times in which each iteration starts from the previous solution. This may increase the computational complexity and latency of the searching algorithm.

The literature review discussed above have led a research momentum at a recent time turning into investigation in throughput and spectral efficiency (SE) of massive MIMO downlink transmissions with low mean squared deviation (MSD) receiver. In [53], potential of massive MIMO are discussed from different transceiver design aspects, and two hybrid precoding transceiver architectures are proposed as cost-effective alternatives for combining a digital precoder and an analog precoder. A follow-up study in [54] compares the performance of massive MIMO and cooperative MIMO in a multi-cell environment. Promising results demonstrated by these researches have recently attracted more research interest into massive MIMO systems with low mean-squared deviation (MSD) receivers. Propagation environments with slow and fast fading, different levels of channel coherence and interference have been studied in [54]. Despite interesting researches for mmWave mobile communication, the channel model considered at aforementioned researches does not consider the effect of Doppler shift due to the end users' mobility. Doppler shift can cause crucial disturbances to the received signal and, if not addressed, can greatly degrade communications performance [55]. Therefore [6] introduced a novel channel model with the incorporation of Doppler shift considering a time-domain correlative channel and its related effects on mmWave propagation channel.

B. MAJOR CONTRIBUTIONS

A novel channel model for mobile mmWave massive MIMO systems have been proposed by [6], where the number of clusters and rays generated from each cluster is taken as variables due to the mobility of users. Such channel model have not been studied for mmWave massive MIMO communications before. In the existing literatures, power constraint optimization (PCO) was studied with respect to two conventional schemes that are total power constraint (TPC) and uniform power constraint (UPC). However TPC and UPC have major drawbacks with respect to fairness and achieving QoS for users in dense networks. Thus this paper proposes a novel PCO technique, called as allied TPC and UPC (APC), that aims to harmonize TPC and UPC to achieve optimum system performance with preserving fairness. Further APC considers the novel mmWave channel model proposed by [6]. To handle the user mobility, three optimal beam tracking schemes, conventional exhaustive search (CES), multiobjective joint optimization codebook (MJOC) and linear hybrid combiner (LHS) scheme, have been provided for the mobile mmWave massive MIMO system with the proposed APC scheme. COR and BER performance analysis for the proposed schemes have been provided. These analyses can be very useful for practical applications and radio engineering since they can be used to obtain performance projections easily for various scenarios. The major contributions of this paper can be listed as follows;

- To achieve optimum data rate, a lemma with proof for the solution of the optimization problem in the context of APC is presented with the closed-form expression of the optimal covariance matrix. We also verify the performance of the proposed joint power constraint scheme for the SE and the instantaneous interfering power by comparing the results with the conventional TPC and UPC based optimization respectively. For the proposed APC, the closed form expressions of BER metric analysis have been derived, and then analyzed theoretically and computationally for PCSI and IPCSI case studies.

- The COR analysis mainly important in today's heterogeneous network model due to its potential to safeguard co-existing users no matter even if any part of the channel is already shared to other users. Most of the literature review and research work on the utilization of spectrum have been done based on duty cycle (DC) rather than exploring COR regardless of its importance and potential. Hence we examined COR by proposing DC based COR estimation analysis for the first time in this work and the results showed that COR estimation with DC selection is more effective than both the traditional estimation and the probabilistic model estimation.
- We extend the investigation of beam tracking schemes for mobile mmWave MIMO communications, presented in [6], by introducing conventional exhaustive search (CES) along with multi-objective joint optimization codebook (MJOC) scheme and linear hybrid combiner (LHC) scheme for the proposed APC optimization. Compared to [6], the analytical part of the MJOC scheme is extended with a theorem for the necessary and sufficient condition to hold the inequality and an algorithm for joint optimization codebook design. The performance comparison of three schemes has been performed for the SE and the instantaneous interfering power respectively.

The rest of the paper is organized as follows. Section II describes use of proposed APC scheme in the system model. Section III is presenting channel COR estimation analysis, where three schemes such as traditional COR estimation, probabilistic model based COR estimation and duty cycle (DC) based COR estimation have been compared. Section IV is one of the most important technical parts of this paper, where analytical part of the BER performance for imperfect and perfect CSI is established. Section V is introduced in order to compare and track the performance of various codebook-based schemes. Furthermore, numerical and simulation results are analyzed and discussed in Section VI. Finally, the entire work is concluded in section VII to increase the readability. The key notations and their descriptions used in the paper are listed in Table 1.

TABLE 1. The notations of essential network parameters.

Symbol	Description
B_{T_x}	Number of antenna elements at T_x
B_{R_x}	Number of antenna elements at R_x
d_1	Distance between the user and the first antenna element in a row
d_2	The separation distance between two neighboring antenna elements
$Z(t)$	Number of discovered clusters at time t
v	Velocity
f_c	Carrier frequency
c_s	Speed of light
$\theta(a,t,z)$	The angle between arriving wave and and the direction of motion
Δz	z^{th} cluster's angle of arrival offset
d_3	Distance between the user and the BS
f	The expected value of Doppler frequency shift with respect to z
T_s	Sampling period
M	Number of symbols in a single data frame
α	Path-loss exponent
K	shape parameter
h_a	Rician fading effect
β_a	Arbitrary phase shift
l	Taps in the mmWave channels
C	Number of sub-carriers
τ	Delay
ϵ	Spatial streams
b	Number of beams
x	Number of clusters in each beam
W	Allocated transmission spectrum to each of the spatial streams
R_{sum}	Sum-rate
$H_{i,j}[c]$	The channel matrix between the i^{th} antenna element and the j^{th} user at subcarrier c
J	Number of users
P	Power allocation matrix
$F[c]$	Baseband precoding matrix
$F_{RF}[C]$	RF precoding matrix
$G[c]$	combining matrix
$G_{RF}[c]$	RF combining matrix
Q and Q_0	Input covariance matrix and optimal covariance matrix respectively
P_{tot}	Total power budget
P_i	Allocated power to each of the elements at T_x
I	Identity matrix
λ	Lagrangian multiplier
A	Diagonal matrix
c_c	Observation count
μ and δ	Discrete relaxation parameters, given by 40.(a) and 40.(b) respectively

II. SYSTEM MODEL

Suppose the end users are not static and undergo a high speed mobility. The downlink (DL) signal from BS to the receivers will undergo a Doppler shift due to the receiver's mobility. Doppler shift effects have been extensively studied by widely used channel models. However, at massive MIMO systems user mobility will also have considerable effect on the number of clusters and number of rays generated from each cluster for a transmission. For a multi-antenna system with B antenna elements and the separation distance of d_2 between two neighboring antenna elements, denote $Z(t)$ as the number of discovered clusters at time t and $z = \{1, 2, \cdots, Z(t)\}$ as the index of the cluster. The Doppler frequency shift due to velocity v in the context of antenna element $a \in \{1, 2, \cdots, B\}$ can be expressed by [6],

$$f(a,t,z) = \frac{f_c v}{c_s} \cos\theta(a,t,z), \tag{1}$$

where f_c denotes carrier frequency at which signal modulation occurs, c_s denotes speed of light, $\theta(a,t,z)$ is the angle between arriving wave via the z^{th} cluster at the a^{th} antenna element and the direction of motion, given by (see 3GPP TS36.104) $\cos\theta(a,t,z) = \frac{d_1+ad_2+\Delta z-vt}{\sqrt{(d_1+ad_2+\Delta z-vt)^2+d_3^2}} \approx \frac{d_1+\Delta z-vt}{\sqrt{(d_1+\Delta z-vt)^2+d_3^2}}$ for $d_1 \gg ad_2$ which shows that $\cos\theta(a,t,z)$ will be almost same for all a in such a case. Δz is the z^{th} cluster's angle of arrival offset with respect to an arriving

wave with a single cluster that is taken as a perpendicular wave. $\Delta z \sim \mathbb{U}(1, 2\pi)$, where $\mathbb{U}$ denotes uniform distribution. d_1 denotes distance between the user and the first antenna element in a row, d_3 denotes distance between the user and the BS. Note that at (2), parameters a, t, and z are independent of each other and Doppler frequency shift can be averaged over them one by one. For the mathematical tractability of the analysis, without loss of generality, let $\bar{f} = \mathbb{E}[f(a, t, z)]$ be the expected value of Doppler frequency shift with respect to z.

All the antenna elements apart from multi-antenna arrangement system can be simultaneously capable of receiving the signal, hence the message signal can be modulated with the sampling period T_s resulting M_s symbols in a single data frame. Therefore, MIMO channel with Rician fading effect at the m^{th} symbol can be modelled as [6]:

$$\mathcal{H}_{i,j}(m) = \frac{1}{B}\sum_{a=1}^{B}\frac{h_a}{d_a^{\alpha}}e^{j2\pi\bar{f}mT_s}H_{i,j}(\tau, t), \quad \forall m = \{1, 2, \cdots, M\}, \tag{2}$$

where $B = B_{T_x}$ which signifies a BS denoted as T_x is equipped with B_{T_x} number of antennas, α denotes Path-loss exponent, $d_a = d_1 + ad_2$, $\frac{1}{d_a^{\alpha}}$ denotes path-loss, $h_a = \sqrt{\frac{K}{K+1}}e^{j\varphi_a} + \sqrt{\frac{K}{K+1}}u_a = r_a e^{j\beta_a}$ in which $u_a \sim \mathcal{CN}(0, 1)$ and K denotes shape parameter. r_a follows the Rician distribution with the centre 1 and arbitrary phase shift β_a due to propagation of the signal is uniformly distributed over $[0, 2\pi]$

Based on the MIMO channel response given in [6], the channel matrix between the i^{th} antenna element and the j^{th} user at subcarrier c can be expressed as,

$$H_{i,j}[c] = \sum_{\tau=0}^{l-1}\mathcal{H}_{i,j}(\tau)\exp\{-j\left(\frac{2\pi c}{C}\right)\tau\}, \tag{3}$$

where $l \leq l_c + 1$ is the l^{th} tap in the mmWave channels, C denotes total number of sub-carriers.

At MIMO communications the cross-beam interference can be fully avoided subject to the condition that the total number of antennas at the transmitter is greater than or equal to the total number of antennas at the receiver. In order to compute the maximum throughput, the throughput of a beam is generally estimated as a function of ϵ spatial streams. The MIMO channel throughput from the i^{th} antenna element to the j^{th} user at subcarrier c in DL $\forall j = \{1, 2, \cdots, J\}$ belongs to p^{th} $\forall p = \{1, 2, \cdots, x\}$ cluster of q^{th} $\forall q = \{1, 2, \cdots, b\}$ beam, can be expressed as in (4), as shown at the bottom of the page, where b stands for the total number of beams, x is the number of clusters in each beam, J represents the number of users. W is the allocated transmission spectrum to each of the spatial streams, and b_q denotes beamforming vector associated with the j^{th} user.

$P_{i,j}[c]$ is the power allocated for the transmission over the c^{th} subcarrier from the i^{th} antenna element to the j^{th} user. Then $R_j = \sum_{c=1}^{C}\sum_{i=1}^{B_{R_x}} R_{i,j}[c]$ is the total data rate achieved by the j^{th} user and the total channel sum-rate and transmission power can be given as,

$$R_{sum} = \sum_{j=1}^{J} R_j, \quad \text{and } P_{tot} = \sum_{j=1}^{J} P_j, \tag{5}$$

where $P_j = \sum_{i=1}^{B_{T_x}}\sum_{c=1}^{C} P_{i,j}(c)$ represents the total power allocated for the j^{th} user.

The data rate of far user (FU) is an important concern in practice that cannot be guaranteed in most of the cases. Hence to address this issue and guarantee the fairness among all users we consider Jain's fairness index[1] [64] which represents a normalized quantity and used to measure the fairness of the resource allocation across different areas of the cell in a comprehensive manner. It can be expressed as below,

$$J_{FI} = \frac{\left[\sum_{j=1}^{J} R_j\right]^2}{J\sum_{j=1}^{J} R_j^2}, \quad R_j \geq 0, \tag{6}$$

The optimization problem formulation for the multi-user MIMO channel throughput can be expressed as below,

$$\max_{\{P, F[c], F_{RF}[C]\}} \sum_{j=1}^{J} R_j, \tag{7}$$

where $P = \{P_{i,j}[c], \forall i, \forall j, , \forall c\}$ represents the power allocation matrix.

subject to:

- $\sum_j^J H_{i,j}[c]F[c]F_{RF}[C] \leq P_{tot}$, when total power constraint (TPC) is assumed at the transmitting end, 7.(a);
- $\sum_j^J H_{i,j}[c]Q_{ii}F[c]F_{RF}[C] \leq \frac{P_{tot}}{B_{T_x}}$, when uniform power constraint (UPC) is assumed at the transmitting end, where $F[c]$ stands for a baseband precoding matrix with the dimension $B_{RF} \times B_s$, and $F_{RF}[C] \in \mathbb{C}^{B_{T_x} \times B_{RF}}$ is used to denote the RF precoding matrix, $Q_{ij} = 0^{J\times J}$, $i \neq j$, denotes constraint for i^{th} transmit antenna element and it also signifies that other than ii^{th} element, i.e. $Q_{ii} = 1$, all the other elements are zero of dimension $J \times J$. If uniform power allocation is considered to all the B_{T_x} antenna elements, then $P_i = \frac{P_{tot}}{B_{T_x}}$ $\forall i$; 7.(b).

[1]The Jain's fairness index ranges between 0 and 1. When J_{FI} approaches to 1 the resource allocation in view of users is fair, while values approaching to $\ll 1$ correspond unfair resource allocation.

$$R_{i,j}[c] = \epsilon W \log_2\left(1 + \frac{|P_{i,j}[c]H_{i,j}[c]b_q|^2}{\sum_{q=1}^{b}\sum_{p=1}^{x}\sum_{u=j+1, u\neq j}^{J}|P_{i,u}[c]H_{i,u}[c]b_q|^2 + \sigma^2}\right), \tag{4}$$

- In addition, each antenna element constraint can be adjusted to adapt for some power resilience to a specific antenna element, hence proposing an intermediate solution between the two extreme case power constraint optimization schemes. By combining 7.(a) and 7.(b), an APC based optimization problem formulation can be proposed as follows:

For the considered multi-user MIMO system, the mutual information as a function of an input covariance matrix, i.e. $Q_{i,j}$, can be expressed by [56],

$$\mathbb{M}(s; X_j) = \log_2 det(I + H_{i,j}[c]Q_{ij}H_{i,j}^H F[c]F_{RF}[C]), \quad (8)$$

where $s \sim \mathcal{CN}(0, Q)$.

The optimum data rate under APC is given by,

$$\max_{\substack{\{Q_{i,j}\geq 0,\\ tr(Q_{i,j})\leq P_{tot},\\ diag(Q_{i,j})\leq \frac{P_{tot}}{B_{T_x}}\}}} \log_2 det(I + H_{i,j}[c]Q_{i,j}H_{i,j}[c]^H F[c]F_{RF}[C]), \quad (9)$$

where *det* denotes determinant to capture the associated information about the matrix.

The solution of the optimization problem (9) under $\text{rank}(H) = B_{T_x}$ can be established complying with the proposed lemma 1.

Lemma 1: In order to achieve optimum data rate with the proposed joint optimization constraint, the optimal covariance matrix, i.e., Q_o can be written by,

$$Q_o = L^{-1}(L\hat{A}_o L - I_{B_{T_x}})_+ L^{-1}, \quad (10)$$

where $L \triangleq \sqrt{H_{i,j}[c]H_{i,j}[c]^H}$ and $\hat{A}_o$ can be obtained from the solution of optimization problem as given below,

$$\begin{aligned} &\max_{\hat{A}} \log_2 det[I_{B_{T_x}} + (L\hat{A}L - I_{B_{T_x}})_+], \\ &\text{subject to : } \hat{A} > 0 \\ &\qquad tr[L^{-1}(L\hat{A}L - I_{B_{T_x}})_+ L^{-1}] = P_{tot} \\ &\qquad diag[L^{-1}(L\hat{A}L - I_{B_{T_x}})_+ L^{-1}] \leq \frac{P_{tot}}{B_{T_x}} \end{aligned} \quad (11)$$

Proof: In general, Lagrangian multipliers are applied to derive the sensitivity of the problem formulation for the data rate optimization with respect to the equality and inequality constraints. Thus,

$$\begin{aligned} \mathcal{L}(Q_{i,j}) = &\log_2 det(I_{B_{R_x}} + H_{i,j}[c]Q_{i,j}H_{i,j}^H G[c]G_{RF}[c]) \\ &+\lambda[tr(Q_{i,j}) + P_{tot}] + tr(E(Q_{i,j} - P_i)) \\ &-tr(DQ_{i,j}), \end{aligned} \quad (12)$$

where *tr* is used to denote trace of a square matrix.

The Karush–Kuhn–Tucker (KKT) conditions can be written as follows,

$$\begin{aligned} H^H(I_{B_{R_x}} + H_{i,j}[c]Q_{i,j}H_{i,j}^H G[c]G_{RF}[c])^{-1}H \\ = \lambda I_{B_{T_x}} + E - D, \end{aligned}$$

Subject to: $\lambda \geq 0$,

$$\begin{aligned} &\text{Diagonal } E \geq 0, \\ &\text{Hermitian } D, Q_{i,j} \geq 0, \\ &DQ_{i,j} = 0, \\ &E(\text{diag}(Q_{i,j} - P_i)) = 0, \\ &\lambda[tr(Q_{i,j}) - P_{tot}] = 0, \\ &diag(Q_{i,j}) \leq P_i, \\ &tr(Q_{i,j}) \leq P_{tot}; \end{aligned} \quad (13)$$

where $(\lambda I_{B_{T_x}} + E)$ denotes the positive-definite diagonal matrix as

$$\begin{aligned} &(\lambda I_{B_{T_x}} + E)_{ii} \\ &= \lambda + \lambda_i \\ &= \Psi_i^H (I_{B_{R_x}} + H_{i,j}[c]Q_{i,j}H_{i,j}^H G[c]G_{RF}[c])^{-1}\Psi_i + (D)_{ii} \\ &\geq \Psi_i^H (I_{B_{R_x}} + H_{i,j}[c]Q_{i,j}H_{i,j}^H G[c]G_{RF}[c])^{-1}\Psi_i \\ &> 0. \end{aligned} \quad (14)$$

Some of the inequality properties can be presented as follows:

$$D_{ii} \geq 0, \text{ as } D \geq 0$$

$I_{B_{R_x}} + H_{i,j}[c]Q_{i,j}H_{i,j}^H G[c]G_{RF}[c] > 0$, as $Q_{i,j} \geq 0$. Thereafter, the diagonal matrix can be expressed as,

$$A \triangleq \lambda I_{B_{T_x}} + E > 0 \quad (15)$$

The second inequality property hold for $\Psi_i \neq 0$.

From (13), we get

$$\begin{aligned} &H_{i,j}^H (I_{B_{R_x}} + H_{i,j}[c]Q_{i,j}H_{i,j}^H G[c]G_{RF}[c])^{-1}H_{i,j} \\ &\qquad \times Q_{i,j} = AQ_{i,j}, \end{aligned} \quad (16)$$

$$\text{Subject to : Diagonal} A > 0, \quad (16.a)$$

$$\text{diag}(Q) \leq P_i, \quad (16.b)$$

$$tr(Q_{i,j}) \leq P_{tot}. \quad (16.c)$$

In order to meet the necessary conditions that 16.(c) and Q_o must satisfy equality and inequality (i.e. $tr(Q_o) < P_{tot}$), respectively, the covariance matrix $(Q(\Phi))_{i,j}$ can be expressed by

$$(Q(\Phi))_{i,j} \triangleq \left(\frac{P_i}{(Q_o)_{ii}}\right)^{\frac{\Phi}{2}} Q_{i,j} \left(\frac{P_j}{(Q_o)_{jj}}\right)^{\frac{\Phi}{2}}. \quad (17)$$

The following properties can be observed,

$(Q(\Phi))_{i,j} \geq 0$

$(Q(0))_{i,j} \equiv Q_o$ and $(Q(1))_{i,j} > Q_o$ as $(Q_o)_{i,i} < P_i$ for $1 \leq i \leq B_{T_x}$, else $tr(Q_o) = \sum_{i=1}^{B_{T_x}} Q_{ii} = \sum_{i=1}^{B_{T_x}} P_i \geq P_o$ as $(Q_o)_{ii} = P_i$, $\forall i = \{1, 2, \cdots, B_{T_x}\}$. Therefore, the following can be defined,

$$\delta(\Phi) \triangleq tr[Q(\Phi)] = \sum_{i=1}^{B_{T_x}} \left(\frac{P_i}{(Q_o)_{ii}}\right)^{\Phi} (Q_o)_{ii}. \quad (18)$$

It can be noticed that $\delta(\Phi)$ is a monotonic function of Φ and also strictly increasing for $\Phi \geq 0$.

Furthermore, $\delta(0) = tr(Q_o) < P_{tot}$ and $\delta(1) = \sum_{i=1}^{B_{T_x}} P_i > P_{tot}$ by the considerations.

Thus, $\delta(\hat{\Phi}) = P_{tot}$ and $Q(\hat{\Phi}) > Q_o$ for $\hat{\Phi} \in \{0, 1\}$ meet the TPC with equality and which in turn help to achieve a higher mutual information,

$$\log det(I_{B_{R_x}} + H_{i,j}[c]Q_{i,j}(\hat{\Phi})H_{i,j}^H G[c]G_{RF}[c]) > \log det(I_{B_{R_x}} + H_{i,j}[c]Q_o H_{i,j}^H G[c]G_{RF}[c]). \quad (19)$$

Thereby, to find the data rate, the problem formulation in (16) can be expressed by

$$H_{i,j}^H(I_{B_{R_x}} + H_{i,j}[c]Q_{i,j}H_{i,j}^H G[c]G_{RF}[c])^{-1}H_{i,j}Q_{i,j} = AQ_{i,j}, \quad (20)$$

Subject to: Diagonal$A > 0$, (20.a)

$$\text{diag}(Q) \le P_i, \quad (20.b)$$

$$tr(Q_{i,j}) \le P_{tot}, \quad (20.c)$$

where $Q_{i,i} < P_i$ must be satisfied for only one index from the given range, $1 \le i \le B_{T_x}$.

However, (20) can further extend as follows,

$$\begin{aligned} &HA^{-1}H_{i,j}^H(I_{B_{R_x}} + H_{i,j}[c]Q_{i,j}H_{i,j}^H G[c]G_{RF}[c])^{-1} \\ &\quad H_{i,j}Q_{i,j}H^H = HQ_{i,j}H^H HA^{-1}H_{i,j}^H H_{i,j}Q_{i,j}H^H \\ &\overset{(a)}{=} HQ_{i,j}H^H(I_{B_{R_x}} + H_{i,j}[c]Q_{i,j}H_{i,j}^H G[c]G_{RF}[c])SPP \\ &\quad + P^2, \end{aligned} \quad (21)$$

The notation (a) is used to denote the following equivalence,

$$\begin{aligned} L &\triangleq \sqrt{H_{i,j}[c]H_{i,j}[c]^H} \\ \hat{A} &\triangleq A^{-1} \\ S &\triangleq L\hat{A}L \\ P &\triangleq LQ_{i,j}L \end{aligned}$$

According to [60, Th.1.3.12], we can have,

$$\begin{aligned} S &= L\hat{A}L = UE_S U^H \\ P &= LQ_{i,j}L = UE_P U^H, \end{aligned}$$

where U stands for unitary matrix, whereas E_S and E_P are used to denote diagonal matrices.

Hence, (21) can be further be expressed as,

$$E_S E_P = E_P + E_P^2. \quad (22)$$

Now, $E_P = (E_S - I_{B_{T_x}})_+$ can be computed for the known E_S.

The diagonal position can be chosen anywhere for the given equation,

$$\lambda_S\lambda_P = \lambda_P + \lambda_P^2 = (1 + \lambda_P)\lambda_P. \quad (23)$$

Thus, $\lambda_S \ge 0$ and $\lambda_P \ge 0$ as $Q_{i,j} \ge 0$ and $\hat{A} > 0$.

As we are optimizing the mutual information, we have considered $\lambda_S > 1$ as it provides the solution $\lambda_P = \lambda_S - 1$ and ignored $\lambda_S \le 1$ as it can provide $\lambda_P = 0$ only that is not viable at all. Hence, the feasible solution is $\lambda_P = (\lambda_S - 1)_+$.

As L is non-singular, we get

$$\begin{aligned} Q_o &= L^{-1}U(E_S - I_{B_{T_x}})_+ U^H L^{-1} \\ &= L^{-1}(S - I_{B_{T_x}})_+ L^{-1} \\ &= L^{-1}(L\hat{A}L - I_{B_{T_x}})_+ L^{-1}, \end{aligned} \quad (24)$$

this confirms that (10) belongs to Lemma 1 and which in turn helps to conduct optimization problem given in (11).

III. CHANNEL OCCUPANCY RATIO (COR) ESTIMATION ANALYSIS

The measurement for COR estimation is corresponding to how near the stair case values are to the true values. Besides, it is beneficial to signalize the unoccupied of white space for cognitive radio (CR) networks. False alarm probability, denoted by P_f, is considered here as a design parameter that has great impact on the estimation, hence it is important to be incorporated for better COR estimation. The performance of the COR estimation is followed by the samples of Y observations. The notations φ and $\hat{\varphi}$ are used to denote the true COR and the estimated COR, respectively.

A. TRADITIONAL COR ESTIMATION

The traditional COR estimation is computed based on the ratio of observation count, denoted by c_c, that is higher than the threshold to the total sample number, denoted by Y and can be given by

$$\hat{\varphi} = \frac{c_c}{Y}. \quad (25)$$

B. PROBABILISTIC MODEL BASED COR ESTIMATION

For the given signal to interference plus noise ratio (SINR) and unity probability of detection (i.e.,$P_d = 1$), one can compute the maximum likelihood estimator (MLE) of φ. It is worth-noting that higher value of P_f due to instantaneous COR may cause higher P_d. We have considered $P_d = 1$ only for the analytical derivation of MLE, although it has been again computed by the input signal with unknown P_d.

Therefore, MLE with the assumption $P_d = 1$ can be expressed by

$$\hat{\varphi}(c_c) = \max_{\substack{\{Q_{i,j}\ge 0,\\ tr(Q_{i,j})\le P_{tot},\\ diag(Q_{i,j})\le \frac{P_{tot}}{B_{T_x}}\\ \hat{\varphi}\in[0,1]\}}} \left[\binom{Y}{c_c}\left[(1-\hat{\varphi})P_f + \hat{\varphi}\right]^{c_c} \times \left[1 - (1-\hat{\varphi})P_f - \hat{\varphi}\right]^{Y-c_c}\right]. \quad (26)$$

Now, by $\frac{d\hat{\varphi}(c_c)}{d\hat{\varphi}} = 0$ we get

$$\hat{\varphi}(c_c) = \frac{\frac{c_c}{Y} - P_f}{1 - P_f} \quad (27)$$

To avoid negative value of $\hat{\varphi}$, the following hypotheses are assumed,

$$\hat{\varphi}(c_c) = \begin{cases} \frac{\frac{c_c}{Y} - P_f}{1 - P_f}; & c_c \ge YP_f \\ 0; & c_c < YP_f, \end{cases} \quad (28)$$

The above assumption is treated as instantaneous COR approach. In order to obtain maximum allowable P_f, we can have the coefficients for the truncated Gaussian variables as below,

$$a_1 = -\frac{1}{Y(P_f - 1)}, \tag{29}$$

$$a_0 = \frac{P_f}{P_f - 1}. \tag{30}$$

According to [58], the coefficients for the truncated Gaussian variables are as follows, $a_1 = \frac{1}{M}$ and $a_0 = 0$

C. DUTY CYCLE (DC) BASED COR ESTIMATION

Detecting the existence of the wanted signal can be represented as a binary decision, by $\beta^c_{t,b}$ which can be evaluated based on the comparison between strength of the received signal,$P^c_{t,b}$, and the detection threshold, $\gamma^c_{t,b}$.

Thus,

$$\beta^c_{t,b} = \begin{cases} 1; & P^c_{t,b} > \gamma^c_{t,b} \\ 0; & else, \end{cases} \tag{31}$$

where, $t = \{1, 2, \cdots, T_s\}$ denotes the sweep time index, $b = \{1, 2, \cdots, n\}$ denotes the frequency bin index. The DC estimation at b can be defined by [59]

$$\Psi^c_b = \frac{1}{T_s} \sum_{t=1}^{T_s} \beta^c_{t,b}. \tag{32}$$

The detection probability can be measured with the help of the probability mass function (PMF) of $T_s\Psi^c_b$, which signifies the binomial random variable with probability of success. The PMF for $\max_{b\in\Omega_h} T_s\Psi^c_b$ can be calculated by the process of taking away a CDF value from the successive CDF value. Hence, by applying the ratio of success count (t_{sc}) to T_s as a weight to the PMF, we can define the COR as

$$\hat{\varphi}(\varpi, \Omega_h) = \sum_{t_x=1}^{T_p} \frac{t_x}{T_s} \Bigg(\prod_{c\in\Omega_h} F\left(t_x, T_p, P^{\varpi}_{\beta,b}\right) - F\left(t_x - 1, T_p, P^{\varpi}_{\beta,b}\right) \Bigg), \tag{33}$$

where ϖ corresponds to single threshold or double-threshold approaches, Ω_h denotes number of frequency bins in each channel, F is used to denote PMF and $T_p = \varphi T_s$.

IV. BIT ERROR RATE (BER) PERFORMANCE ANALYSIS FOR IMPERFECT AND PERFECT CHANNEL STATE INFORMATION (CSI)

For the assumption of maximal ratio combining (MRC) at the receiving end, the decision parameter can be given by

$$\xi_{i,j}[c] = \sum_{i=1}^{B_{R_x}} \Bigg(\frac{G^*[c]G^*_{RF}[c]H_{i,j}[c]F[c]F_{RF}[c]\hat{H}^H_{i,j}[c]s[c]}{||\hat{h}[c]||^2} + \frac{(G^*[c]G^*_{RF}[c]\omega[c])\hat{H}^H_{i,j}[c]}{||\hat{h}[c]||^2} \Bigg), \tag{34}$$

where $\hat{h}[c]$ denotes channel estimation at the c^{th} subcarrier, $\hat{H}^H_{i,j}[c] = H_{i,j}[c] + \varepsilon_{i,j}[c]$ [60] and $\varepsilon_{i,j} \sim \mathcal{CN}(0, \sigma_\varepsilon)$. $\varepsilon_{i,j}[c]$ is the Gaussian error and also independent and identically distributed (i.i.d.), and has a zero-mean with variance σ_ε. Therefore, BER at the c^{th} subcarrier can be defined by

$$p_e = P_r\{Re\{\xi_{i,j}[c]\} > 0 | s[c] = -\sqrt{E_s}\}, \tag{35}$$

where E_s denotes energy per modulation symbol.

Therefore, the quadratic form (QF) of a random variable (RV) V_r can be expressed by

$$V_r = \sum_{i=1}^{B_{R_x}} S_{i,j}[c] M_q S^H_{i,j}[c], \tag{36}$$

where QF matrix M_q and RV vector $S_{i,j}[c]$ can be expressed as follows,

$$S_{i,j}[c] \triangleq \begin{bmatrix} X_{i,j}[c] \\ \hat{H}_{i,j}[c] \end{bmatrix}, \quad M_q \triangleq \begin{bmatrix} 0 & -\frac{1}{2} \\ -\frac{1}{2} & 0 \end{bmatrix}. \tag{37}$$

By using (36) and (37), we can further extend (35) to

$$p_e = P_r \Bigg\{ \sum_{i=1}^{B_{R_x}} \left(X_{i,j}[c]\hat{H}^H_{i,j}[c] + X^H_{i,j}[c]\hat{H}_{i,j}[c] \right) < 0 | s[c] = -\sqrt{E_s} \Bigg\}. \tag{38}$$

By considering the mean vector $v_{i,j} \triangleq \mathbb{E}\{S_{i,j}[c]\}$ and the covariance matrix $Q_{i,j} \triangleq \mathbb{E}\left\{ \left(S_{i,j} - v_{i,j}\right)\left(S^H_{i,j} - v^H_{i,j}\right) \right\}$, we can further have

$$\begin{aligned} v_{i,j} &= \epsilon_{dc}\kappa(\varsigma)U, \\ Q_{i,j} &\triangleq \begin{bmatrix} c_{11} & c_{12} \\ c_{21} & c_{22} \end{bmatrix} \\ &= \begin{bmatrix} |s[c]|^2 + \sigma^2_\omega\ (1 - \sigma^2_\varepsilon)s[c] & \\ (1 - \sigma^2_\varepsilon)s^H[c]\ 1 - \sigma_\varepsilon \end{bmatrix}, \end{aligned} \tag{39}$$

where ϵ_{dc} denotes complex-valued direct current (DC) offset,

$$\kappa(\varsigma) = \sqrt{C}\frac{sinc(c + \varsigma)}{sinc(\frac{c+\varsigma}{C})} \exp\left\{ -j\pi(c + \varsigma)\frac{(C - 1)}{C} \right\},$$

$$sinc(y) = \frac{sin(\pi y)}{\pi y}, \quad U^T = [1\ 0].$$

A. CASE STUDY I

Under the non-ideal condition, the closed form expression of the BER for imperfect CSI (IPCSI) can be determined by [61],

$$p_e = \frac{1}{2} + \sum_{i=0}^{B_{R_x}-1} q_i(\mu) J_i(\bar{\epsilon}^2_c \delta^2) e^{-\bar{\epsilon}^2_c \varrho^2}, \tag{40}$$

where $J_i(.)$ denotes i^{th} order hyperbolic Bessel functions of the 1^{st} kind, $\bar{\epsilon}_c = \sqrt{\sum_{i=1}^{B_{R_x}} |\epsilon_{dc}\kappa(\varsigma)|^2}$, and μ, δ and $q_i(\mu)$ are

given by,

$$\mu = \left| \frac{(tr(Q_{i,j}M_q) + \sqrt{tr(Q_{i,j}M_q)^2 - 4det(Q_{i,j}M_q)})}{(tr(Q_{i,j}M_q) - \sqrt{tr(Q_{i,j}M_q)^2 - 4det(Q_{i,j}M_q)})} \right|, \tag{40.a}$$

$$\delta = \sqrt{\frac{1}{2}\frac{c_{22}}{tr(Q_{i,j}M_q)^2 - 4det(Q_{i,j}M_q)}}), \tag{40.b}$$

$$q_i(\mu) = \frac{a}{(1+\mu)^{2B_{R_x}-1}} \sum_{x=0}^{B_{R_x}-1-i} \binom{2B_{R_x}-1}{x} \times[\mu^x - \mu^{2B_{R_x}-1-x}]; a = \begin{cases} \frac{1}{2}, & i = 0 \\ 1, & i \neq 0. \end{cases} \tag{40.c}$$

B. CASE STUDY II

Under the ideal condition, the closed form expression of the BER for perfect CSI (PCSI) can be determined by [62],

$$p_e = \frac{1}{2}\left[1 - \sum_{i=0}^{B_{R_x}-1} \Gamma J_0\left(\Gamma^2 \frac{|\epsilon_{dc}\kappa(\varsigma)|^2}{2E_s}\right) \exp\left\{-\Gamma^2 \frac{|\epsilon_{dc}\kappa(\varsigma)|^2}{2E_s}\right\}\right], \tag{41}$$

where $\Gamma = \sqrt{\frac{\bar{\gamma}}{1+\bar{\gamma}}}$ and $\bar{\gamma} = \frac{E_s}{\sigma_\omega^2}$.

Now, assuming $\bar{\gamma} \to \infty$, $|\epsilon_{dc}\kappa(\varsigma)|^2 \ll E_s$ and by the linear approximation of p_e with the help of the first-order Taylor polynomial we can simplify (40) as below,

$$p_e \approx \frac{|\epsilon_{dc}\kappa(\varsigma)|^2}{4E_s}. \tag{42}$$

According to [65, refer to (13.3-7)], we can have another simplified form of expression for BER as

$$p_e = \frac{1}{2}(1 - \Gamma) \tag{43}$$

By substituting (43) into (42), we get

$$|\epsilon_{dc}|^2 = \frac{4E_s}{|\kappa(\varsigma)|^2}(1 - \Gamma) \tag{44}$$

V. CODEBOOK-BASED BEAM TRACKING SCHEMES

In the framework of beamspace based massive MIMO communication with mobile users, UEs' locations in the orthogonal subspace is the main criterion in order to achieving the optimum response. The UEs' channels which, although literally correlated in the radio propagation, are nevertheless requiring advanced beam tracking schemes to deal with channel correlation in optimizing the performance of the wireless communication systems. The object of this investigation in this section has evolved into the analysis of quantitative assessment with the commonly used design performance metrics, namely sum-rate, for comparing and tracking the performance of various codebook-based schemes.

A. CONVENTIONAL EXHAUSTIVE SEARCH (CES) SCHEME

A spatial Fourier transform matrix (SFTM) can be used to represent the conventional antenna space as a beamspace. Let's denote M_1 and M_2 as the SFTM for T_x and R_x, respectively. M_1 and M_2 are an orthogonal set of steering vectors and can be expressed as,

$$\begin{aligned} M_1 &= [g(\Psi_1), \cdots, g(\Psi_{B_{T_x}})], \\ \text{and } M_2 &= [g(\Psi_1), \cdots, g(\Psi_{B_{R_x}})], \end{aligned} \tag{45}$$

where $g(\Psi_{n_1})\forall n_1 \in \{1, \cdots, B_{T_x}\}$ and $g(\Psi_{n_2})\forall n_2 \in \{1, \cdots, B_{R_x}\}$ are the steering vectors that can be expressed as,

$$\begin{aligned} g(\Psi_{n_1}) &= \frac{1}{\sqrt{B_{T_x}}} \exp(-j\pi\Psi_{n_1}), \\ \text{and } g(\Psi_{n_2}) &= \frac{1}{\sqrt{B_{R_x}}} \exp(-j\pi\Psi_{n_2}), \end{aligned} \tag{46}$$

where $\Psi_{n_1} = \frac{1}{B_{T_x}}\left(n - \frac{(B_{T_x}+1)}{2}\right)$ and $\Psi_{n_2} = \frac{1}{B_{R_x}}\left(n - \frac{(B_{R_x}+1)}{2}\right)$ are pre-defined spatial directions.

The beamspace channel matrix can be expressed as,

$$\begin{aligned} \bar{H} &= M^H H_{i,j} \\ &= [M^H H_{i,1}, \cdots, M^H H_{i,B_{RF}}] \\ &= [\bar{H}_{i,1}, \cdots, \bar{H}_{i,B_{RF}}], \end{aligned} \tag{47}$$

where $M = M_1 M_2$ and $H_{i,j}, \forall j \in \{1, \cdots, B_{RF}\}$ is the beamspace channel vector of the j^{th} UE.

At training phase a reduced dimension matrix $\bar{H}_\kappa \in \mathbb{C}^{B_{RF}\times B_{RF}} = \bar{H}(b,:)_{b\in K}$ for a BS with B_{RF} UEs, needs to be rebuilt, where $K = [I_1, \cdots, I_{B_{RF}}]$ represents the preferred beams cardinality and $I_{B_{RF}} = E\{mm^H\}$ for the signal vector to B_{RF} UEs denoted by $m \in \mathbb{C}^{B_{RF}\times 1}$. Hence after dividing by s[c], (1) in [6] can again be re-expressed as,

$$X^E[c] = G^E[c]\bar{H}_k^H[c]F^E[c] + \omega^E[c] \tag{48}$$

where $(.)^E$ denotes the resultant matrix from conventional exhaustive search (CES) algorithm. Further, γ_j and R_j given by (4) can be updated accordingly. By exploiting the channel sparsity, the sum-rate can be optimized with the beam selection as follows, let

$$\bar{H}_k^{opt} = \arg\max_K R_{sum}, \tag{49}$$

by linear mapping (49) can be

$$\bar{H}_k^{opt} = \arg\max_K tr\left((\bar{H}(b,:)_{b\in K}^H \bar{H}(b,:)_{b\in K})^{-1}\right). \tag{50}$$

The greatest absolute entry in (48) results in optimum beams. Substituting (50) into (48), the best beam-pair can be determined and the optimal solution to CES is found. It should be noted that channel sparsity at MIMO cannot be available at all scenarios. The considered case of mmWave channel and massive MIMO beamforming helps with channel sparsity since at mmWave channel there are generally only a few reflected path that prevents a rich scattering environment and are from a limited subset of all angular directions, i.e. small

angular spread. Also the large antenna array of massive MIMO helps with differentiating directions with signals and directions without signals that in turn helps with utilizing spatial sparsity. Reference [65] studied the sparsity property of wireless channels through real-world measurement and pointed out that using the assumption that wireless channels are widely sparse has pitfalls and should be done only for appropriate scenarios. Although CES provides a direct-forward approach to find optimal beams, it becomes computationally infeasible as the codebook size increases. Thus we propose MJOC and LHC schemes to provide computationally feasible solutions for optimal beam tracking.

B. MULTIOBJECTIVE JOINT OPTIMIZATION CODEBOOK (MJOC) SCHEME

Multiobjective joint optimization with the novel proposed power optimization constraint, APC, is a challenging problem that needs a number of problem transformations to become computationally feasible. Inequality theorem, sparse signal approximation for best problem matching and iterative optimization algorithm is introduced in this section to achieve a feasible solution.

This leads to the following theorem,

Theorem: A necessary and sufficient condition to hold the desired inequality, i.e., $|\tilde{Q}_{s_1,s_2}| \leq |\tilde{Q}_{s_1,s_1}|, \forall s_1 \neq s_2$, is the optimal solution of $\max_{\mu_j,\delta_j,Q_{s_1,s_2}} \sum_{j=1}^{J} \delta_j R_j + \Xi||F||_\infty^2$ [refers to (20) in [6]], i.e., $\{\tilde{\mu}_j, \tilde{\delta}_j, \tilde{Q}_{s_1,s_2}\}$.

Proof: Suppose that $Q_j = Q_{j,j}, \forall j$ and $V(x,y) = \max_j |Q_j(x,y)|, \forall x, y$. The condition,'rank $(Q_{s_1,s_2}) = 1, \forall s_1, \forall s_2$,' [refers to 20(b) in [6]] is non-convex according to [63], hence given problem formulation can be extended with the exclusion of non-convex condition to

$$\max_{\{\mu_j,\delta_j,Q_j\},V} \sum_{j=1}^{n} \delta_j R_j + \Xi tr\left(1_{B_{T_x}\times B_{T_x}} V\right), \tag{51}$$

$$\text{Subject to : } 1+\mu_j \geq e^{\delta_j}, \sum_{j=1}^{J} tr\left(\hat{F}_{RF} Q_{j,j}\right) \leq P_{max}, \tag{51.a}$$

$$\gamma_j \geq \mu_j, \gamma_j \geq \hat{\delta}_j, Q_j \succeq 0, V \geq |Q_j|, \quad \forall j. \tag{51.b}$$

In order to transform the non-convex condition $\gamma_j \geq \mu_j, \gamma_j \geq \hat{\delta}_j, \forall j$, we further reformulate (51) with the inclusion of additional metrics η_j and Θ_j into

$$\max_{\{\mu_j,\delta_j,Q_j,\eta_j,\Theta_j\},V} \sum_{j=1}^{n} \delta_j R_j + \Xi tr\left(1_{B_{T_x}\times B_{T_x}} V\right), \tag{52}$$

$$\text{Subject to: } \eta_j^2 \leq tr(\hat{X}_j), \hat{Q}_j \succeq 0, 1+\mu_j \geq e^{\delta_j}, \quad \forall j, \tag{52.a}$$

$$\sum_{u=1,u\neq j}^{n} tr(\hat{X}_u) + \sigma^2 \leq \Theta_j,$$

$$\sum_{j=1}^{n} tr\left(\hat{F}_{RF} Q_j\right) \leq P_{max}, \quad \forall j, \tag{52.b}$$

$$\sum_{u=1,u\neq j}^{n} \hat{\delta}_j \left(tr(\hat{X}_u) + \sigma^2\right) \leq tr(\hat{X}_j),$$

$$\frac{\eta_j^2}{\Theta_j} \geq \mu_j, \quad \forall j, \tag{52.c}$$

where $\frac{\eta_j^2}{\Theta_j} \geq \mu_j$ is a non-convex constraint. The successive convex approximation (SCA) technique [2] is used to decompose this inequality and express it as follows,

$$\frac{\eta_j^2}{\Theta_j} \geq \Lambda_j^{(f)}(\eta_j, \Theta_j) \triangleq 2\frac{\eta_j^{(f)}}{\Theta_j^{(f)}}\eta_j - \left(\frac{\eta_j^{(f)}}{\Theta_j^{(f)}}\right)^2 \Theta_j, \quad \forall j, \tag{53}$$

where the notation $(.)^{(f)}$ is used to represent the f^{th} iteration of the SCA technique. In order to achieve a convex solution, (52) is re-expressed as,

$$\max_{\{\mu_j,\delta_j,Q_j,\eta_j,\Theta_j\},V} \sum_{j=1}^{n} \delta_j R_j + \Xi tr\left(1_{B_{T_x}\times B_{T_x}} V\right),$$

$$\text{Subject to : } 52.(a), 52.(b), \sum_{u=1,u\neq j}^{n} \hat{\delta}_j \left(tr(\hat{X}_u) + \sigma^2\right)$$

$$\leq tr(\hat{X}_j), \quad \forall j \text{ and } \Lambda_j^{(f)}(\eta_j, \Theta_j) \geq \mu_j, \ \forall j. \tag{54}$$

This concludes the proof. Algorithm 1 provides the optimal codebook design by keeping Ξ constant and setting $\varnothing$ as the objective function. Suppose $\Upsilon^{(f)}$ defines the cardinality of all the metrics used in (54) at the f^{th} iteration. Algorithm 1 is given as:

Algorithm 1 Joint Optimization Codebook Design

1. Initialization: $f = 0$, generate feasible initial points $\Upsilon^{(f)}$ and evaluate $\varnothing^{(f)}$.
2. **for** $|\varnothing^{(*)} - \varnothing^{(f)}| \leq \Xi$ **do**
3. Convexify the problem (54) with $\Upsilon^{(f)}$
4. Update: $f \leftarrow f+1$, $\varnothing^{(*)} \leftarrow \varnothing^{(f)}$, $\Upsilon^{(*)} \leftarrow \Upsilon^{(f)}$
5. Optimized output: $\Upsilon^{(*)}$, $\varnothing^{(*)}$
6. **end for**

In order to improve the performance at the short training blocks regime keeping the target of lower-complexity receivers design in mind, we require a hybrid combiner with low mean squared deviation (MSD) between the transmitted and received signals.

It has been shown by [63] that MJOC's performance may be limited when the number of beamforming vectors at T_x and/or combining vectors at R_x is limited. That is the reason why we propose the LHC scheme next, as an ideal scheme for such scenarios.

TABLE 2. The main simulation parameters [6].

Parameter	Value	Parameter	Value
User's velocity	20m/s	Distance from BS to users	40m
Data rate	133 Mbps	Number of BSs	32
Wavelength	0.15m	Channel coherence	64 blocks
Doppler frequency	133Hz	Normalized doppler frequency	10^{-6}

C. LINEAR HYBRID COMBINER (LHC) SCHEME

LHC scheme is based on the MSD minimization principle where the average squared difference (distance) between the estimated values and the actual value are minimized. MSD has an advantage over other distance based measures as it is analytically tractable. The LHC scheme is presented in [6] with analytical derivations and shown the minimum MSD problem as below,

$$(G^*, G^*_{RF}) = \arg \min_{\substack{G\in\mathbb{C}^{B_{RF}\times B_s},\\ G_{RF}\mathbb{C}^{B_{R_x}\times B_{RF}}}} \Big[tr\{\xi ||\mathbb{E}[XX^H]^{\frac{1}{2}} (G^H_{MSD} - G^H G^H_{RF})||^2_F\} - \log_2 \xi \Big], \quad (55)$$

where $||.||^2_F$ denotes the standard Frobenius norm and (55) indicates to observe the prediction of G_{MSD} without a limitation over the cardinality of $G^H G^H_{RF}$ for $G_{RF} \in \mathbb{C}^{B_{R_x}\times B_{RF}}$. The MSD estimation problem is a joint estimation problem of multiple signal realizations, especially when the signal samples have a joint sparse support over a given constraint. Hence, address the problem by the product of F and F_{RF} as an optimal precoder and determine GG_{RF}. The sparse signal approximation for the best matching projection is given by an algorithm named as 'sparse signal approximation for best matching projection'. The following optimization problem presents an algorithmic solution [6],

$$\min_{\hat{G}} ||\sqrt{\xi}(G_{MSD} - \mathbb{E}[XX^H]G_{RF}\hat{G})||^2_F,$$
$$\text{subject to: } ||diag(\hat{G}\hat{G}^*)||_0 = B_{RF} \quad \text{and } ||\nu^H_{R_x}\hat{G}||^2_F = P_{max}. \quad (56)$$

VI. SIMULATION RESULTS AND DISCUSSION

In this section, numerical results are provided for the developed power constraint optimization, TPC and UPC, and beam tracking schemes. System performance has been evaluated based on the metrics given by (6) for the two conventional practices in power-constraint optimization and the novel proposed power allocation technique, APC.

The aim at optimization is to maximize R_{total}. Also the performance of these schemes with respect to the developed COR and BER analysis are investigated. Table 2 provides the details about the simulation parameters. As CSI is a crucial aspect of reliable high data-rate communications in MIMO channel, perfect CSI at T_x and R_x is assumed at the simulations denoted as PCSI, which serves as the benchmark performance. Also the more practical case of imperfect CSI, denoted as IPCSI, is investigated. In the simulation testbed, CES is established with an iterative linear mapping paradigm which methodically computes all the possible candidates for the optimal solution and decides the best beam-pair. The number of iterations is limited to 50 for the CES in order to keep the computation time and complexity low. MJOC Scheme is developed using a theorem to determine convex solution and then expanding into a multiple objective problem formulation with the application of a joint optimization codebook design algorithm. LHC scheme is obtained with joint estimation of multiple signal realizations and approaching the problem by compiling sparse signal approximation for best matching projection algorithm.

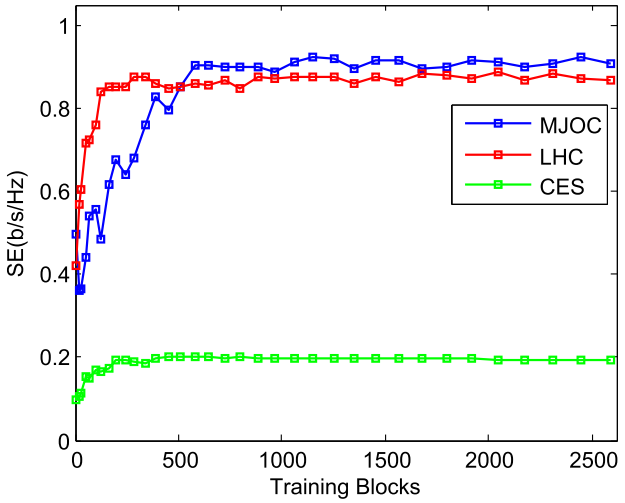

FIGURE 1. SE performance versus training blocks (i.e. number of beamforming vectors at Tx x number of combining vectors at Rx) for CES, MJOC and LHC schemes.

Figure 1 shows the SE performance of CES, MJOC and LHC schemes versus training blocks. Training blocks at beamforming is the number of beamforming vectors at the transmitter side multiplied with the number of combining vectors at the receiver side. CES scheme's performance is shown to be almost independent from the training block size. Although this seems to be an advantage for the cases where training block size is not known or changing during the systems deployment, CES's performance is seen to be inferior to the other studied schemes at all scenarios. Thus CES is not a favorable scheme. It can be seen from the figure LHC scheme outperforms other schemes when training block size is less than 500, i.e. short block size. MJOC scheme outperforms other schemes once the training block size is more than 500, in other words medium to large block size. It is expected that in future communication systems, the block size will be around this range. This is why we focus on the performance of MJOC scheme at the rest of this paper.

Figure 2 shows the SE performance versus number of users at the system for TPC, UPC and APC schemes. It can be seen that APC and TPC schemes performance increases as the number of users in the network increases. This is due

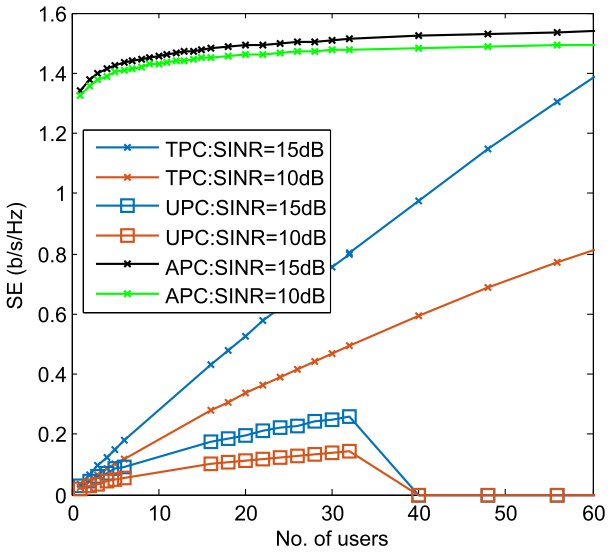

FIGURE 2. SE performance versus the number of users at the system for TPC, UPC and proposed scheme, APC. Here, the assumed training block for beam-tracking equals to 1600.

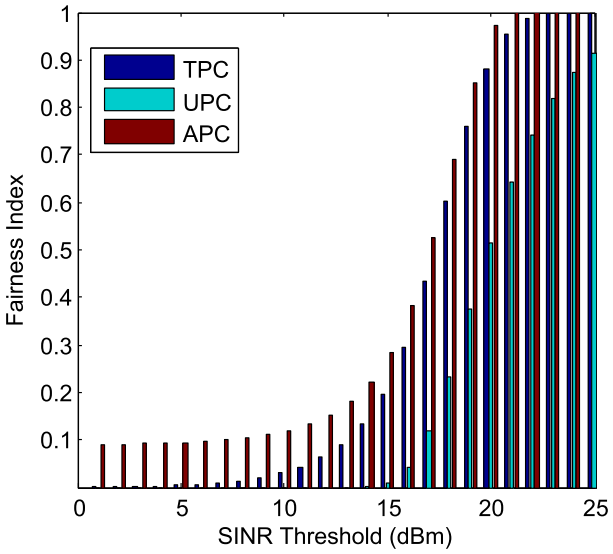

FIGURE 3. Jain's fairness index versus SINR threshold for TPC, UPC and APC schemes. Here the assumed number of users for beam-tracking equals to 20.

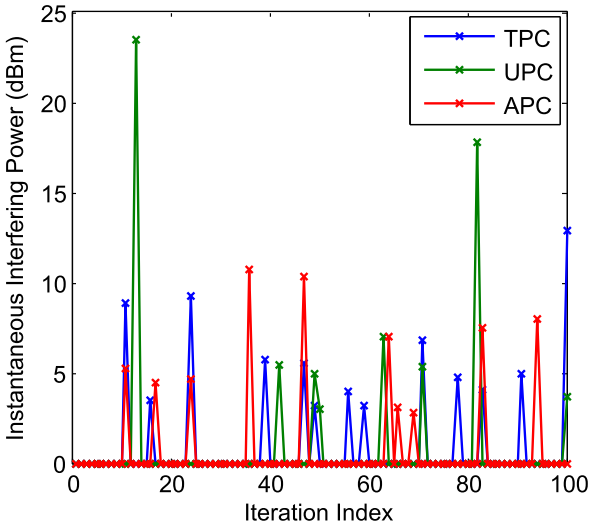

FIGURE 4. Instantaneous interfering power versus iteration index for TPC, UPC and APC schemes.

to multi-user gain. However, for UPC scheme the performance quickly degrades and becomes zero when the network becomes densely populated, i.e. number of users is 40 or more. The reason for this is because UPC scheme tries to provide an equal share of power to all users within the power budget, but the allocated power for each user gets to a level where no users can achieve successful data transmission. This is a major disadvantage of UPC. APC scheme outperforms other schemes for all the considered cases of network density and SINR. This is due to the proposed joint power optimization constraint where the optimal covariance matrix is obtained and solved and the allocation is done accordingly instead of performing the allocation solely with respect to a total or uniform power constraint.

Figure 3 shows the Jain's fairness index [63] with respect to the SINR threshold for TPC, UPC and APC schemes. Employing a scheme that can achieve fairness among user is vital for systems where users are geographically distributed and mobile, and the coverage area have many obstacles, such as high-rise building in an urban area. In case fairness is not addressed, users that have good channel conditions may have high performance where users with worse channel conditions suffer low performance continuously. It can be seen that APC provides better fairness among users for the whole SINR threshold regime of the simulation. Together with performance shown on figure 2, it can be seen that APC can provide better SE while achieving more fairness among users compared to the conventional TPC and UPC schemes. These are crucial performances for a scheme to be employed in practice at future communication networks.

Figure 4 shows the instantaneous interfering power versus iteration index for TPC, UPC and APC schemes. It can be seen that the performance of all the schemes depends on the iteration index, so that in case APC is employed as the scheme for a system, the iteration index can be adjusted to minimize the instantaneous interfering power.

Figure 5 shows the COR estimation versus iteration index for traditional, probabilistic and DC based estimation analysis. The figure shows that highest COR can be obtained by DC based estimation which can help with reducing interference and protect co-channel users. With the higher value of COR, the detection probability for any other users occupying the interested channel is higher. It is expected that in next generation of communication networks there will be more non-orthogonal schemes employed. Thus detecting occupied channels with a high success rate will be even more important.

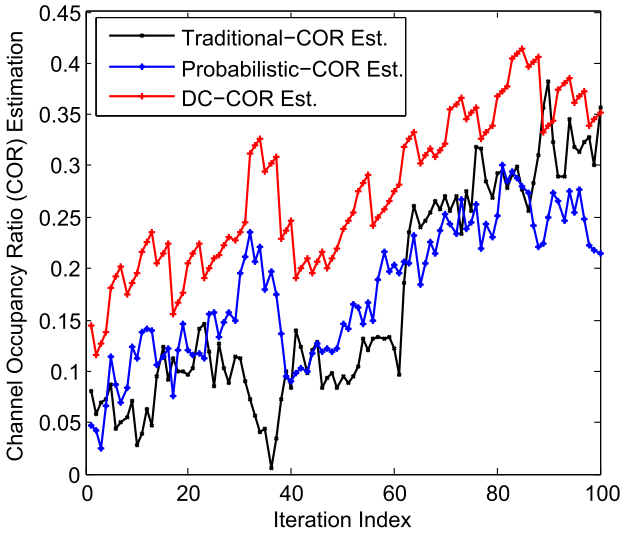

FIGURE 5. COR estimation versus iteration index for traditional, probabilistic and DC based estimation. Here the assumed number of users for beam-tracking equals to 20.

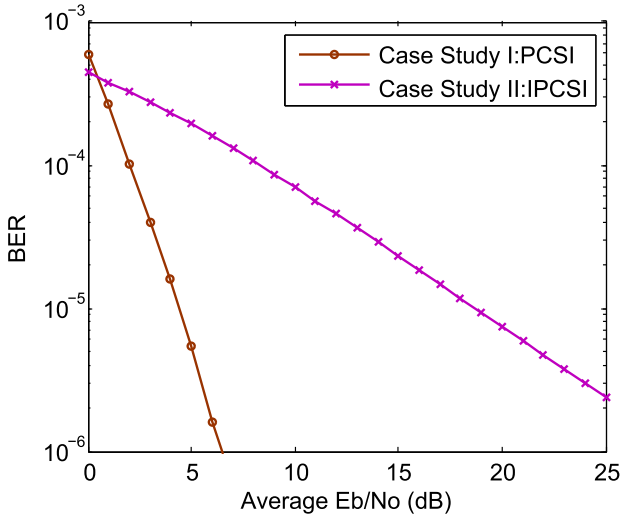

FIGURE 6. BER versus average SNR per bit for PCSI and IPCSI cases.

Figure 6 shows the BER versus averaged SNR per bit performance for PCSI and IPCSI cases. It can be seen that having a perfect CSI information can greatly improve the BER performance compared to IPCSI case and the performance gain increases as the SNR per bit increases. Data critical applications in current and future generation of communication systems may require BER to be as low as 10^{-6}. The figure shows that in PCSI case this value can be achieved. However, when CSI is imperfect the required BER for data critical applications cannot be achieved even with SNR per bit equals to 25 dB. Thus having perfect or highly accurate CSI is crucial in data critical applications of future mobile mmWave massive MIMO based networks. Another advantage of having PCSI is that for a given BER threshold the required SNR per bit will be much less compared to IPCSI case. This can significantly help with the overall system's energy efficiency and reduce cost due to lower power consumption and transceiver amplifier design.

VII. CONCLUSION

This paper proposes a novel power constraint optimization scheme called as APC where the optimal covariance matrix is obtained and the power allocation is done accordingly instead of performing the allocation solely with respect to conventional TPC or UPC. Three optimal beam-tracking schemes - CES, MJOC and LHC - are proposed for mobile mmWave massive MIMO communications with APC. The channel model considered in this paper is new and different from widely used models in that the number of clusters and number of rays within each cluster are varying due to user mobility. Analysis for vital performance metrics BER and COR are provided. Beam-tracking schemes and mathematical derivations for BER and COR consider this new channel model. Three analysis methods are studied for COR metric estimation – traditional, probabilistic and DC based – and it has been shown that DC based estimation outperforms other analysis methods. BER analysis are provided for PCSI and IPCSI cases and it is noted that PCSI can improve the overall system's energy efficiency and reduce cost due to lower power consumption and transceiver amplifier design. SE performance for the beam-tracking and power constraint optimization schemes are investigated. It is concluded that MJOC scheme outperforms other beam-tracking schemes when the training block length is in medium to large scale. Employing MJOC, it is shown that APC scheme can outperform the conventional TPC and UPC for all the considered simulation scenarios.

ACKNOWLEDGMENT

This work is an extended version of the paper titled "A Novel Channel Model and Optimal Beam Tracking Schemes for Mobile Millimeter-Wave Massive MIMO Communications" published in IEEE Transactions on Vehicular Technology, in July 2021, [DOI:10.1109/TVT.2021.3083635].

REFERENCES

[1] Cisco Public. (2020). *Cisco Annual Internet Report (2018–2023) White Paper*. USA, White Paper. [Online]. Available: https://www.cisco.com/c/en/us/solutions/collateral/executive-perspectives/annual-internet-report/white-paper-c11-741490.html

[2] J. Li, C. Gu, Z. Wu, and C. Wu, "Distributed optimization methods for non-convex problems with inequality constraints over time-varying networks," *Complexity*, vol. 2017, pp. 1–10, Jan. 2017, doi: 10.1155/2017/3610283.

[3] N. N. Moghadam, G. Fodor, M. Bengtsson, and D. J. Love, "On the energy efficiency of MIMO hybrid beamforming for millimeter-wave systems with nonlinear power amplifiers," *IEEE Trans. Wireless Commun.*, vol. 17, no. 11, pp. 7208–7221, Nov. 2018.

[4] W.-B. Sun, Q.-Y. Yu, J.-C. Guo, W.-X. Meng, and V. C. M. Leung, "A joint iterative optimal resource allocation algorithm for non-orthogonal multi-user and multi-weight opportunistic beamforming systems," *IEEE Trans. Veh. Technol.*, vol. 69, no. 3, pp. 2864–2877, Mar. 2020.

[5] P. Zhou, X. Fang, and Y. Long, "Throughput and robustness guaranteed beam tracking for mmWave wireless networks," in *Proc. IEEE/CIC Int. Conf. Commun. China (ICCC)*, Oct. 2017, pp. 1–6.

[6] J. Ghosh, H. Zhu, and H. Haci, "A novel channel model and optimal beam tracking schemes for mobile millimeter-wave massive MIMO communications," *IEEE Trans. Veh. Technol.*, vol. 70, no. 7, pp. 7205–7210, Jul. 2021.

[7] W.-Y. Chen, B.-S. Chen, and W.-T. Chen, "Multiobjective beamforming power control for robust SINR target tracking and power efficiency in multicell MU-MIMO wireless system," *IEEE Trans. Veh. Technol.*, vol. 69, no. 6, pp. 6200–6214, Jun. 2020.

[8] Y. Lin, Z. Yang, and H. Guo, "Proportional fairness-based energy-efficient power allocation in downlink MIMO-NOMA systems with statistical CSI," *China Commun.*, vol. 16, no. 12, pp. 47–55, Dec. 2019.

[9] R. Malik and M. Vu, "Optimizing throughput in a MIMO system with a self-sustained relay and non-uniform power splitting," *IEEE Wireless Commun. Lett.*, vol. 8, no. 1, pp. 205–208, Feb. 2019.

[10] J. Tan and L. Dai, "Wideband beam tracking in THz massive MIMO systems," in *Proc. IEEE Global Commun. Conf. (GLOBECOM)* Apr. 2020, pp. 1–6.

[11] S. G. Larew and D. J. Love, "Adaptive beam tracking with the unscented Kalman filter for millimeter wave communication," *IEEE Signal Process. Lett.*, vol. 26, no. 11, pp. 1658–1662, Nov. 2019.

[12] R. Van der Merwe, "Sigma-point Kalman filters for probabilistic inference in dynamic state-space models," Ph.D. dissertation, OGI School Sci. Eng., Oregon Health Sci. Univ., Beaverton, OR, USA, 2004.

[13] S. J. Julier and J. K. Uhlmann, "Unscented filtering and nonlinear estimation," *Proc. IEEE*, vol. 92, no. 3, pp. 401–422, Mar. 2004.

[14] H.-L. Song and Y.-C. Ko, "Robust and low complexity beam tracking with monopulse signal for UAV communications," *IEEE Trans. Veh. Technol.*, vol. 70, no. 4, pp. 3505–3513, Apr. 2021.

[15] C. Zhang, D. Guo, and P. Fan, "Tracking angles of departure and arrival in a mobile millimeter wave channel," in *Proc. IEEE Int. Conf. Commun. (ICC)*, May 2016, pp. 1–6.

[16] S. Kim, H. Han, N. Kim, and H. Park, "Robust beam tracking algorithm for mmWave MIMO systems in mobile environments," in *Proc. IEEE 90th Veh. Technol. Conf. (VTC-Fall)*, Sep. 2019, pp. 1–5.

[17] J. Zhang, W. Xu, H. Gao, M. Pan, Z. Han, and P. Zhang, "Codebook-based beam tracking for conformal array-enabled UAV mmWave networks," *IEEE Internet Things J.*, vol. 8, no. 1, pp. 244–261, Jan. 2021.

[18] Y. Ke, H. Gao, W. Xu, L. Li, L. Guo, and Z. Feng, "Position prediction based fast beam tracking scheme for multi-user UAV-mmWave communications," in *Proc. IEEE Int. Conf. Commun. (ICC)*, May 2019, pp. 1–7.

[19] H.-L. Song, Y.-C. Ko, J. Cho, and C. Hwang, "Beam tracking algorithm for UAV communications using Kalman filter," in *Proc. Int. Conf. Inf. Commun. Technol. Converg. (ICTC)*, Oct. 2020, pp. 1101–1104.

[20] Y. Yapici and I. Guvenc, "Low-complexity adaptive beam and channel tracking for mobile mmWave communications," in *Proc. 52nd Asilomar Conf. Signals, Syst., Comput.*, Oct. 2018, pp. 572–576.

[21] S. Blandino, T. Bertrand, C. Desset, A. Bourdoux, S. Pollin, and J. Louveaux, "A blind beam tracking scheme for millimeter wave systems," in *Proc. IEEE 91st Veh. Technol. Conf. (VTC-Spring)*, May 2020, pp. 1–6.

[22] J. Palacios, D. De Donno, and J. Widmer, "Tracking mm-wave channel dynamics: Fast beam training strategies under mobility," in *Proc. IEEE Conf. Comput. Commun. (INFOCOM)*, May 2017, pp. 1–9.

[23] R. Bacchus, T. Taher, K. Zdunek, and D. Roberson, "Spectrum utilization study in support of dynamic spectrum access for public safety," in *Proc. IEEE Symp. New Frontiers Dyn. Spectr. (DySPAN)*, Apr. 2010, pp. 1–11.

[24] T. Kamakaris, M. M. Buddhikot, and R. Iyer, "A case for coordinated dynamic spectrum access in cellular networks," in *Proc. 1st IEEE Int. Symp. New Frontiers Dyn. Spectr. Access Netw. (DySPAN)*, Nov. 2005, pp. 289–298.

[25] A. D. Spaulding and G. H. Hang, "On the definition and estimation of spectrum occupancy," *IEEE Trans. Electromagn. Compat.*, vol. EMC-19, no. 3, pp. 269-280, Aug. 1977.

[26] K. Umebayashi, T. Kazmi, Y. Kamiya, Y. Suzuki, and J. Lehtomaki, "Dynamic selection of CWmin in cognitive radio networks for protecting IEEE 802.11 primary users," in *Proc. CROWNCOM*, Osaka, Japan, Jun. 2011, pp. 266–270.

[27] J. J. Lehtomäki, R. Vuohtoniemi, K. Umebayashi, and J.-P. Mäkelä, "Energy detection based estimation of channel occupancy rate with adaptive noise estimation," *IEICE Trans. Commun.*, vol. 95, no. 4, pp. 1076–1084, 2012.

[28] E. Arslan, A. T. Dogukan, and E. Basar, "Sparse-encoded codebook index modulation," *IEEE Trans. Veh. Technol.*, vol. 69, no. 8, pp. 9126–9130, Aug. 2020.

[29] A. T. Dogukan and E. Basar, "Super-mode OFDM with index modulation," *IEEE Trans. Wireless Commun.*, vol. 19, no. 11, pp. 7353–7362, Nov. 2020.

[30] M. Abdullahi, A. Cao, A. Zafar, P. Xiao, and I. A. Hemadeh, "A generalized bit error rate evaluation for index modulation based OFDM system," *IEEE Access*, vol. 8, pp. 70082–70094, 2020.

[31] H. Zhu, Z. Cao, Y. Zhao, and D. Li, "Learning to denoise and decode: A novel residual neural network decoder for polar codes," *IEEE Trans. Veh. Technol.*, vol. 69, no. 8, pp. 8725–8738, Aug. 2020.

[32] I. Al-Nahhal, O. A. Dobre, and S. Ikki, "On the complexity reduction of uplink sparse code multiple access for spatial modulation," *IEEE Trans. Commun.*, vol. 68, no. 11, pp. 6962–6974, Nov. 2020.

[33] Y. Fu, C.-X. Wang, X. Fang, L. Yan, and S. Mclaughlin, "BER performance of spatial modulation systems under a non-stationary massive MIMO channel model," *IEEE Access*, vol. 8, pp. 44547–44558, 2020.

[34] Y. Zhao, Y. Xiao, P. Yang, S. Fang, and W. Xiang, "Iterative compensation for clipping noise in spatial modulation OFDM systems," *IEEE Trans. Veh. Technol.*, vol. 68, no. 12, pp. 12422–12426, Dec. 2019.

[35] A. Hilario-Tacuri, J. Maldonado, M. Revollo, and H. Chambi, "Bit error rate analysis of NOMA-OFDM in 5G systems with non-linear HPA with memory," *IEEE Access*, vol. 9, pp. 83709–83717, 2021.

[36] J. Sun, Y. Zhang, J. Xue, and Z. Xu, "Learning to search for MIMO detection," *IEEE Trans. Wireless Commun.*, vol. 19, no. 11, pp. 7571–7584, Nov. 2020.

[37] F. Kalbat, A. Al-Dweik, B. Sharif, and G. K. Karagiannidis, "Performance analysis of precoded wireless OFDM with carrier frequency offset," *IEEE Syst. J.*, vol. 14, no. 2, pp. 2237–2248, Jun. 2020.

[38] Z. Luo, Y. Chen, C. Li, X. Xiong, and L. Zhu, "Minimum BER criterion and adaptive moment estimation based enhanced ICA for wireless communications," *IEEE Access*, vol. 8, pp. 152071–152080, 2020.

[39] Q. Tao, C. Zhong, X. Chen, H. Lin, and Z. Zhang, "Maximum-eigenvalue detector for multiple antenna ambient backscatter communication systems," *IEEE Trans. Veh. Technol.*, vol. 68, no. 12, pp. 12411–12415, May 2019.

[40] Q. Tao, Y. Li, C. Zhong, S. Shao, and Z. Zhang, "A novel interference cancellation scheme for bistatic backscatter communication systems," *IEEE Commun. Lett.*, vol. 25, no. 6, pp. 2014–2018, Jun. 2021.

[41] K. Yang, J. Ren, C. Tian, J. Wang, and H. V. Poor, "Decoding binary linear codes over channels with synchronization errors," *IEEE J. Sel. Areas Commun.*, vol. 38, no. 12, pp. 2853–2863, Dec. 2020.

[42] Z. Chen, L. Zhang, Z. Wu, L. Wang, and W. Xu, "Reliable and efficient sparse code spreading aided MC-DCSK transceiver design for multiuser transmissions," *IEEE Trans. Commun.*, vol. 69, no. 3, pp. 1480–1495, Mar. 2021.

[43] M. Saad, J. Palicot, F. Bader, A. C. A. Ghouwayel, and H. Hijazi, "A novel index modulation dimension based on filter domain: Filter shapes index modulation," *IEEE Trans. Commun.*, vol. 69, no. 3, pp. 1445–1461, Mar. 2021.

[44] M. Zhu, D. G. M. Mitchell, M. Lentmaier, D. J. Costello, and B. Bai, "Error propagation mitigation in sliding window decoding of braided convolutional codes," *IEEE Trans. Commun.*, vol. 68, no. 11, pp. 6683–6698, Nov. 2020.

[45] I. Trigui, E. K. Agbogla, M. Benjillali, W. Ajib, and W.-P. Zhu, "Bit error rate analysis for reconfigurable intelligent surfaces with phase errors," *IEEE Commun. Lett.*, vol. 25, no. 7, pp. 2176–2180, Jul. 2021.

[46] M. A. A. Careem and A. Dutta, "Real-time prediction of non-stationary wireless channels," *IEEE Trans. Wireless Commun.*, vol. 19, no. 12, pp. 7836–7850, Dec. 2020.

[47] A. Gouissem, R. Hamila, N. Al-Dhahir, L. Ben-Brahim, and A. Gastli, "Time-dependent bit error rate analysis for smart utility networks in the presence of WLAN interferers," *IEEE Syst. J.*, vol. 14, no. 2, pp. 2133–2143, Jun. 2020.

[48] S. Srivastava, J. Nath, and A. Jagannatham, "Data aided quasistatic and doubly-selective CSI estimation using affine-precoded superimposed pilots in millimeter wave MIMO-OFDM systems," *IEEE Trans. Veh. Technol.*, vol. 70, no. 7, pp. 6983–6998, Jul. 2021.

[49] P. J. Okoth, Q. N. Nguyen, D. R. Dhakal, D. Nozaki, Y. Yamada, and T. Sato, "An efficient codebook-based beam training technique for millimeter-wave communication systems," in *Proc. Asia–Pacific Microw. Conf. (APMC)*, Nov. 2018, pp. 666–668, doi: 10.23919/APMC.2018.8617193.

[50] V. Va, H. Vikalo, and R. W. Heath, Jr., "Beam tracking for mobile millimeter wave communication systems," in *Proc. IEEE Global Conf. Signal Inf. Process. (GlobalSIP)*, Dec. 2016, pp. 743–747, doi: 10.1109/GlobalSIP.2016.7905941.
[51] L. N. Ribeiro, A. L. F. de Almeida, and J. C. M. Mota, "Separable linearly constrained minimum variance beamformers," *Signal Process.*, vol. 158, pp. 15–25, May 2019, doi: 10.1016/j.sigpro.2018.12.010.
[52] S. Kim, G. Kwon, and H. Park, "High-resolution multi-beam tracking with low overhead for mmWave beamforming system," *ICT Exp.*, vol. 7, no. 1, pp. 28–35, Mar. 2021.
[53] X. Yu, J.-C. Shen, J. Zhang, and K. B. Letaief, "Alternating minimization algorithms for hybrid precoding in millimeter wave MIMO systems," *IEEE J. Sel. Topics Signal Process.*, vol. 10, no. 3, pp. 485–500, Apr. 2016, doi: 10.1109/JSTSP.2016.2523903.
[54] Z. Chen, F. Sohrabi, and W. Yu, "Multi-cell sparse activity detection for massive random access: Massive MIMO versus cooperative MIMO," *IEEE Trans. Wireless Commun.*, vol. 18, no. 8, pp. 4060–4074, Aug. 2019.
[55] C. Zhang, G. Wang, M. Jia, R. He, L. Zhou, and B. Ai, "Doppler shift estimation for millimeter-wave communication systems on high-speed railways," *IEEE Access*, vol. 7, pp. 40454–40462, 2019, doi: 10.1109/ACCESS.2018.2861889.
[56] T. M. Cover and J. A. Thomas, *Elements of Information Theory*. Hoboken, NJ, USA: Wiley, 2006.
[57] R. Horn and C. Johnson, *Matrix Analysis*, 2nd ed. Cambridge, U.K.: Cambridge Univ. Press, 2013.
[58] N. Johnson, S. Kotz, and N. Balakrishnan, *Continuous Univariate Distributions*, vol. 1. Hoboken, NJ, USA: Wiley, 1994.
[59] M. López-Benítez and F. Casadevall, "Methodological aspects of spectrum occupancy evaluation in the context of cognitive radio," *Eur. Trans. Telecommun.*, vol. 21, no. 8, pp. 680–693, Dec. 2010.
[60] S. Zhou and G. B. Giannakis, "How accurate channel prediction needs to be for transmit-beamforming with adaptive modulation over Rayleigh MIMO channels?" *IEEE Trans. Wireless Commun.*, vol. 3, no. 4, pp. 1285–1294, Jul. 2004.
[61] E. Martos-Naya, J. F. Paris, U. Fernandez-Plazaola, and A. J. Goldsmith, "Exact BER analysis for M-QAM modulation with transmit beamforming under channel prediction errors," *IEEE Trans. Wireless Commun.*, vol. 7, no. 10, pp. 3674–3678, Oct. 2008.
[62] J. G. Proakis, *Digital Communications*, 5th ed. New York, NY, USA: Mc Graw-Hill, 2004.
[63] O. Mehanna, N. D. Sidiropoulos, and G. B. Giannakis, "Joint multicast beamforming and antenna selection," *IEEE Trans. Signal Process.*, vol. 61, no. 10, pp. 2660–2674, May 2013.
[64] R. K. Jain, D. M. W. Chiu, and W. R. Hawe, "A quantitative measure of fairness and discrimination for resource allocation in shared computer systems," Eastern Res. Lab., Digit. Equip. Corp., Hudson, MA, USA, Tech. Rep. DEC-TR-301, 1984.
[65] R. He, B. Ai, G. Wang, M. Yang, C. Huang, and Z. Zhong, "Wireless channel sparsity: Measurement, analysis, and exploitation in estimation," *IEEE Wireless Commun.*, vol. 28, no. 4, pp. 113–119, Aug. 2021, doi: 10.1109/MWC.001.2000378.